DESIGN AND OPTIMISATION OF UAV EMPENNAGE FOR VARIOUS MISSION SCENARIOS.

Witold Klimczyk
Warsaw University of Technology
ul. Nowowiejska 24, Warszawa
wklimczyk@meil.pw.edu.pl

Zdobysław Goraj
Warsaw University of Technology
ul. Nowowiejska 24, Warszawa
goraj@meil.pw.edu.pl

Abstract. Aircraft design process is typically aimed to provide the optimal solution for some mission scenario(s). Especially during initial design phases, engineers assume level, straight flight as dominant, and the aircraft performance calculations are based on this assumption. Mission scenarios for UAVs are different, and sometimes consist of significant time spent in climb (e.g. atmosphere research) or turn (observation of fixed point) phases. In this paper, the optimisation incorporating different flight conditions is carried out for the empennage of PW-141.1 "Samonit" aircraft. Two different boom-mounted empennage design arrangements are investigated: V-tail (2 surfaces at some angle) and conventional (horizontal and two vertical surfaces). The objective is to assess the effect of mission scenario on the optimal empennage arrangement, showing which is superior in particular conditions. The objective function in optimisation process is maximisation of the aircraft's performance, defined as maximum lift to drag ratio, which for the empennage design is minimisation of drag. Optimal shape is chosen not only basing on the performance, but also robustness of the design.

Keywords. empennage drag reduction, aerofoil optimisation, robust optimisation, surrogate modelling, Kriging

Symbols.

α	Angle of attack	Re	Reynolds number
c_l	Lift coefficient	ρ	Free stream density
c_d	Drag coefficient	V_∞	Free stream velocity
$F_{i,obj}$	i-th objective function	w_i	i-th weighting of objective function
f_{c_d}	Scaled drag coefficient objective function	y_i	i-th parameter
$f_{s,obj}$	Weighted multi objective function		

1 Introduction

Aircraft performance can be judged in various ways, which typically depend on their mission. For big airliners, what counts, is amount of fuel burnt per passenger, gliders are assessed by endurance and/or range. In case of Unmanned Air Vehicles (UAVs) the most popular mission scenarios are surveillance related [5], which require long endurance and range. Both are inversely proportional to drag coefficient [10], hence, drag minimisation is one of the key aspects during aircraft design process.

The optimisation process goal is an objective function, or if there are many goals- a set of objective functions to be minimised or maximised. In practice all problems have multiple goals [4], however, as it is not possible to consider all at the same time, only more important are investigated. Single objective, empennage drag minimisation problem, results in multiple objectives, when a designer takes into consideration different flight phases. Example Medium-Altitude-Long-Endurance (MALE) UAV drag contribution from empennage, varies between 10% (in straight flight) to 30% (during descent) of total drag [8]. It is clear, that different flight conditions, result in different designs, which minimise drag. To find the one, which results in total drag minimisation, throughout the whole flight, is the real design issue.

Design is said to be robust, when a small perturbation of its parameter value does not cause big change in the performance of this design [13]. This holds for any parameters that can change, not only environment related (e.g. free stream conditions) but also those that define the design geometry. During whole flight, the empennage operates at different conditions, hence robustness of the design has to be assessed.

The parametric definition of empennage would result in at least 20-30 parameters [12], which makes the optimisation very expensive. It is thus reasonable to split the whole optimisation into few problems of lower dimensionality. Such approach limits the chance of finding the real optimum, however, allows better exploration and exploitation of search space [4]. Such a split, in wing optimisation, often separates aerofoil and planform [12].

Aerofoil optimisation is a problem typically tackled by global search methods [7,11,14,15], most commonly genetic algorithms (GA) and Particle Swarm Optimisation (PSO). Local search is not appropriate in this problem area, due to the nature of search space, with number of local minima. Various fidelity solvers can be used to calculate objective function. Starting with low-fidelity X-FOIL [12,15], ending with high-fidelity Reynolds-Averaged-Navier-Stokes (RANS) solver, coupled with turbulence models [7,11,14].

Surrogate modelling driven optimisation is getting increasingly popular, as well as its use to assess design sensitivities [4]. [14] present an approach to robust aerofoil optimisation, which uses surrogate model to establish relationship between Mach number, design variables and aerodynamics. Despite their advantages, response surface methods are, however, still not very popular approach, with only a few attempts to optimise aerofoil. These attempts, however, do not take into account varying conditions.

1.1 PW-141 "Samonit"

Samonit was a project aimed to develop a long-endurance UAV for surveillance purposes [3,4]. The base configuration has the boom-mounted v-shaped empennage (Figure 1). The design of the empennage was constrained by the parachute recovery system, requiring space between two booms. This design was created for border surveillance, which results in mission scenario not involving many manoeuvres. However, if the same aircraft was used for different mission type, involving more turning or ascending/descending, v-tail would be less appropriate, and classical empennage with separate vertical and horizontal surfaces would probably be a better choice.

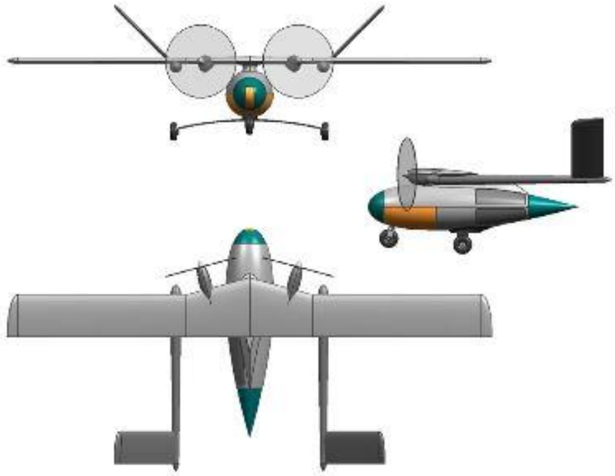

Figure 1 Base configuration of PW141 „Samonit“.

In the current paper, the robust design process of aerofoil, used for the empennage of the aircraft in the MALE class, is presented. Two cases are examined: symmetric aerofoil (used for vertical stabiliser or for v-tail), and asymmetric aerofoil (used for tailplane). The first case is aimed at finding the design which minimises drag, taking into account different angles of attack. The second case aims at finding Pareto front for drag minimisation, and lift-to-drag ratio maximisation. The process is driven by surrogate modelling of moderately expensive, high-fidelity RANS calculations, coupled with turbulence model. The usefulness of such approach to aerofoil optimisation is examined, by comparing results, with some widely used NACA aerofoils.

2 Optimisation of symmetric aerofoil

Symmetric wing, as a vertical stabiliser, is always a part of conventional empennage, it can be also used for v-tail. Because symmetric wing is based on symmetric aerofoil, this was the first step in empennage design optimisation. The process of optimisation guided by surrogate modelling performed in the current follows a framework on Figure 2. During the first stage following aspects are defined:

1. **Fixed parameters**. These are the parameters that will not be changed during optimisation. The actual engineering problem does not have fixed parameters, however, without some simplifications the problem would become too complex. In case of aerofoil optimisation, the chord is assumed constant (1m) and free stream condition was defined.
2. **Objective function(s)**. Symmetric aerofoil optimisation in the current paper only finds a design which minimises drag.
3. **Constraints**. In case of aerofoil optimisation the number of constraints can be defined, including structure and flight mechanics related. In this work an aerofoil which minimises drag will be searched and compared to NACA0010. For this reason aerofoils with sufficient (10% chord) thickness will be considered. Constraints, however, can be approached in various ways, e.g. penalty functions [16], and inevitably lead to multidisciplinary problem (structure-aerodynamics-flight mechanics coupling). A fixed constraint can eliminate a design which in overall would be the best (even though it breaches the constraint). For this reason no designs were eliminated due to constraint violation, however, those that breach it are appropriately marked.

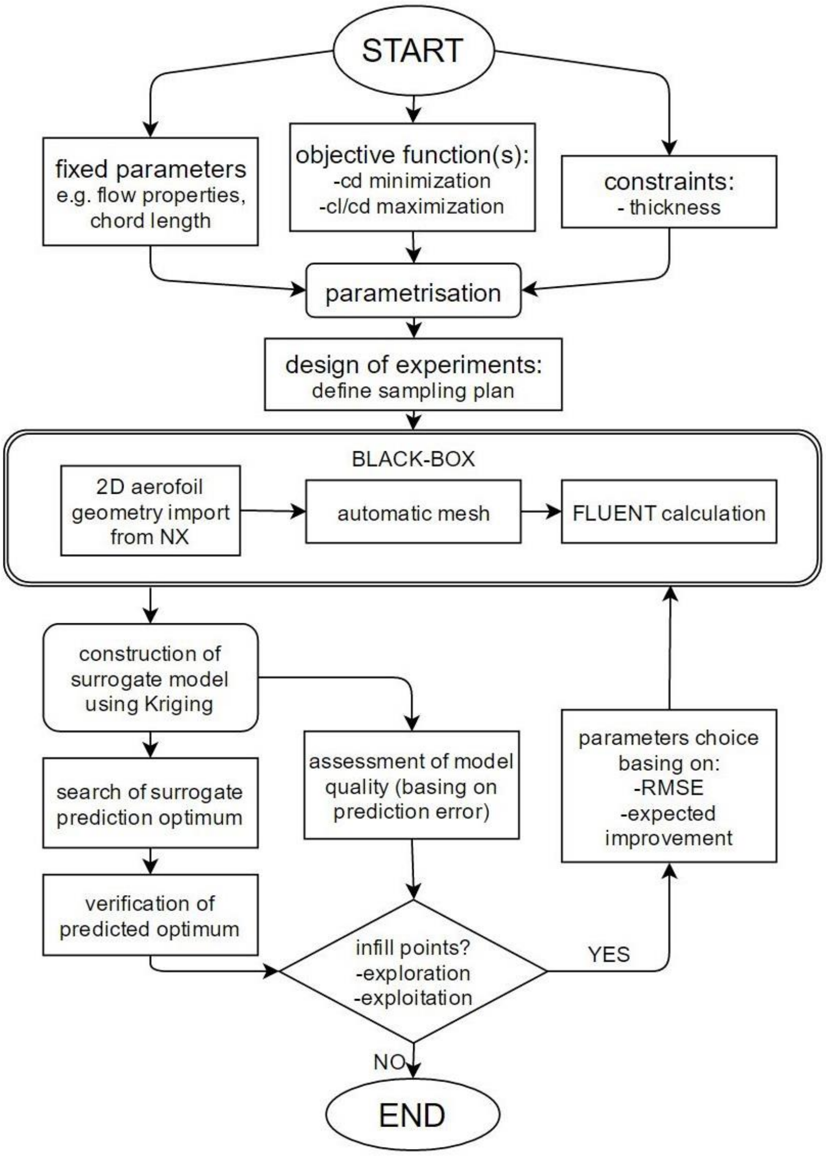

Figure 2 Aerofoil optimisation framework.

2.1 Parametrisation

Aerofoil parametrisation can be done in many ways, most commonly used are PARSEC [17] and NURBS [11], which define top and bottom curves with at least 10 parameters. In this paper an intuitive 4-parameter parametrisation, basing on NX spline, was adopted. NX creates geometry of the spline by construction of non-uniform rational B-spline curve (NURBS) taking as inputs coordinates of poles. The weight of each pole in this optimisation was the same, so the spline definition is reduced to ordinary B-spline curve. NURBS approach was investigated, and the choice of four points resulted from a trade-off between simple shape curves, defined by low number of points, and unrealistic, “bumpy” curves resulting from adding more poles. Aerofoil does not require extremely complicated curvature definition, and the most important features can be controlled with parameterisation used.

Four parameters describing the shape, are coordinates of four guide points (spline poles), in the direction perpendicular to chord (y-axis). Positions along the chord (x-axis) were fixed. Continuity at the leading edge was assured by the first pole location, above the leading edge. This pole defines leading edge curvature. Poles 2 and 3 were located at 20% and 40% of chord and their y-coordinate define curvatures of the surface, imply the position and magnitude of maximum thickness. Pole 4 defines trailing edge angle and the rear curvature.

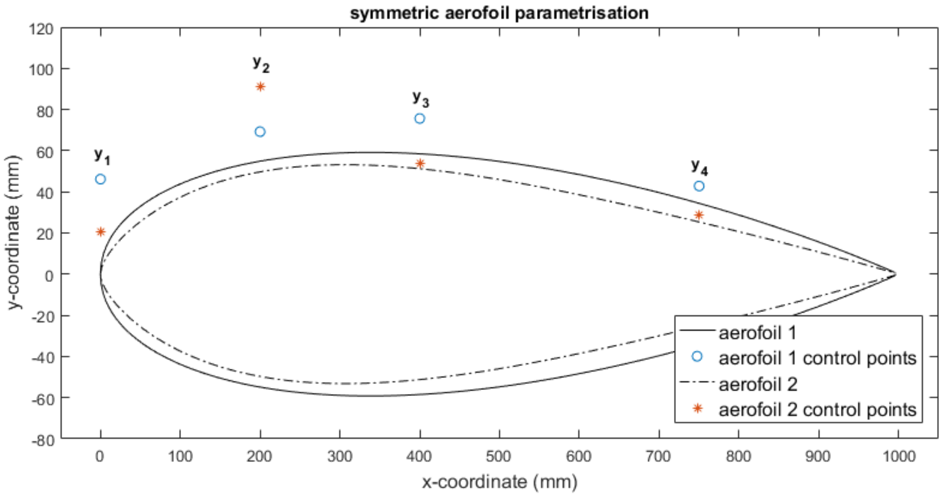

Figure 3 Symmetric aerofoil parametrisation using 4 parameters.

	$y_1\ (mm)$	$y_2\ (mm)$	$y_3\ (mm)$	$y_4\ (mm)$
Lower limit (LL)	20	50	50	10
Upper limit (UL)	50	100	100	50

Table 1 Upper and lower limits of design variables.

Described parametrisation allows to construct some known (e.g. NACA00xx) profiles (with some tolerance) and many more, as the poles locations are continuous (in defined range) and independent.

Both design of experiments and optimisation is performed in scaled variables, i.e. between 0 and 1. The conversion between actual and scaled values is made using Equation (1).

$$Scaled = \frac{Actual - LL}{UL - LL} \tag{1}$$

Boundary conditions are specified to roughly meet the ‘Samonit’ MALE case. For the analysis, free stream velocity was $30\ m/s$ and the chord was $1m$. This gave $Re = 2\ \times 10^6$. This choice does not limit the generality of the approach- any shock-free problem can be approached (shock can result in non-smooth c_d variation to input parameters).

2.2 Design of experiments

Creating a good quality surrogate model, with limited number of experiments, requires adequate choice of the set of experiments. As suggested by Forrester et al. [3], the approach of Morris and Mitchell *maximin* Latin hypercube sampling technique, which ensures good space-filling, was used in this work. The MATLAB code used to generate initial sample comes from the optimisation toolbox [2]. The size of initial sample is dictated by experience and suggests to sample $10n$ points [3], where n is number of parameters- 40 points were sampled in 4 design variables.

2.3 Black-box

Black-box is a function, which takes 4 input parameters and returns drag coefficient (c_d). The optimisation process in this paper assumed black-box returned values without an error, which is a bold assumption, however, the whole process of design optimisation is only used to guide toward optimum design. Following steps were within black-box:

1. Parameters conversion to aerofoil geometry.

   This was achieved using NX spline. The spline was defined as NURBS, basing on poles coordinates (input parameters).

2. Automatic mesh generation procedure for all geometries.

   Structured C-mesh was created accordingly to instructions described in [7] to ensure good quality mesh for all geometries. This technique provides fine mesh in the areas around aerofoil and in the wake. The mesh was refined to obtain grid independence.

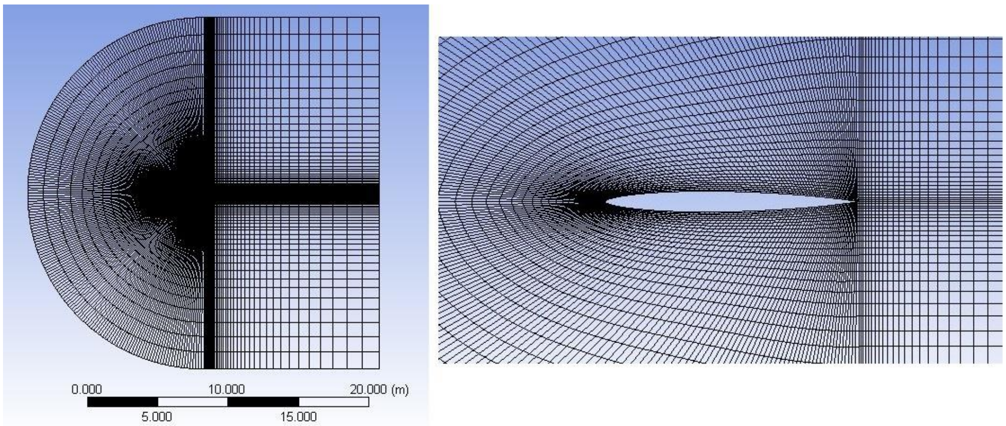

Figure 4 Automated mesh for sample aerofoil: whole mesh (left) and mesh around aerofoil (right).

3. Calculation of resulting forces in *Fluent*.

   This step was the most expensive in the whole optimisation, as each case required around 2000 iterations for convergence. Flow was defined as air at sea level with $\rho = 1.225\frac{kg}{m^3}, V_\infty = 30\frac{m}{s}$. K-ε turbulence model was coupled with RANS equations, to account for all profile drag constituents. The result provided information about forces and their nature (pressure, viscosity).

The results are accompanied by visualisation of pressure distribution at various angles of attack (Figure 5).

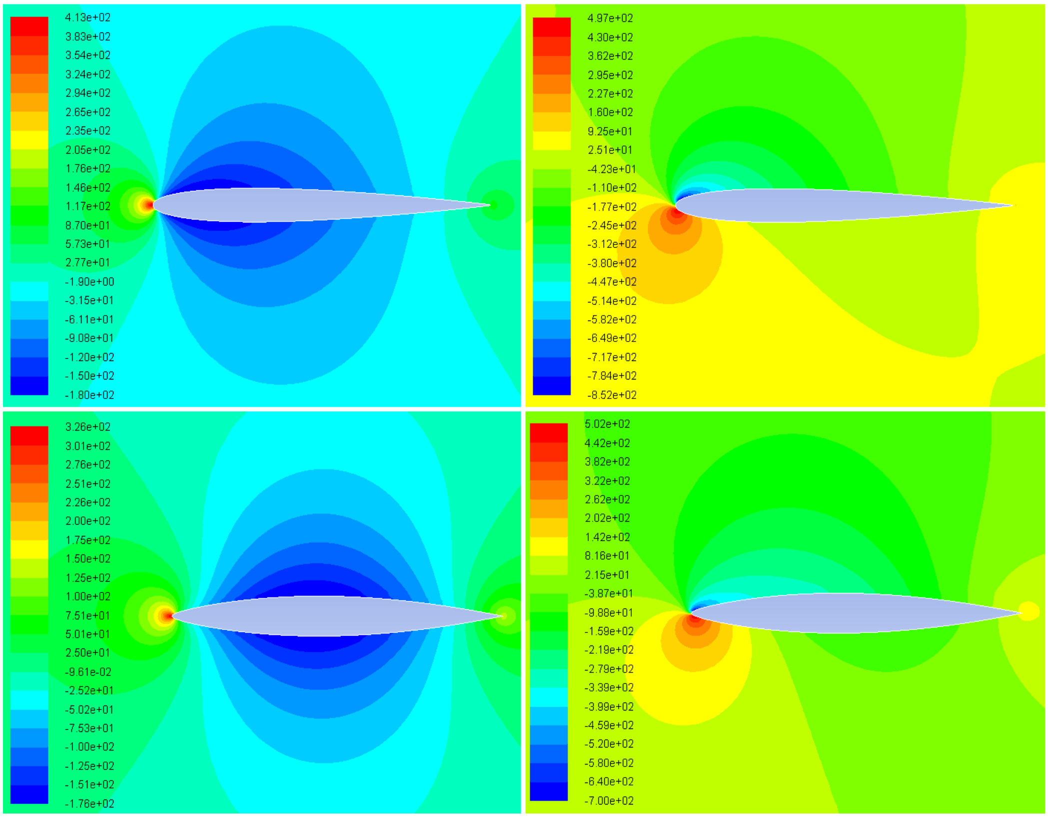

Figure 5 Pressure distributions for NACA0010 (top) and sample (bottom) aerofoils, at zero (left) and 5° (right) angles of attack.

2.4 Weighting

The objective function, taking into account various angles of attack, is of the form:

$$F_{obj} = \min\left[\sum_{i=\alpha}^{n} w_i \times c_d(y_1, y_2, y_3, y_4)_i\right], \tag{2}$$

where i denotes angle of attack and n is number of angles of attack taken into consideration. Finding the optimum requires appropriate choice of weights w_i to account for conditions implied by mission scenario. The choice of weights in this report was not aimed at finding exact values, but rather showing the general impact of this choice on design. In the optimisation process, there is a trade-off between number of angles of attack, at which experiments are performed, which directly influences number of direct black-box function evaluations, and the accuracy of the surrogate model. In this report only 2 angles of attack were taken: $\alpha = 0$ and $\alpha = 5°$. The choice of more intermediate angles of attack is possible, however, drag raise is nearly linear in this regime, and can be accounted for, using the chosen ones. 40 black-box function evaluations were made for each α, as defined by sampling plan.

2.5 Surrogate modelling

After the set of results is obtained the surrogate model was constructed. Construction of surrogate model allows to analyse results with limited data, and prediction of the drag coefficient for any input parameters, basing on statistical prediction. Surrogate model was constructed using MATLAB toolbox which was developed in [2], available to download, following the procedure:

1. Start with defined sampling plan and set of observations for each point.
2. Calculate parameters needed for construction of surrogate model using Kriging [2].

3. Search the surrogate model for predicted optimum using genetic algorithm.

All the assumptions needed for good quality surrogate model [1,2] were satisfied, i.e. continuous design variables, smooth nature of the problem (i.e. no gradual change to observation as any design variable slightly changes).

2.6 Robustness

The robustness of aerofoil design in this work is understood as drag change dependence on the angle of attack, i.e. a robust design is not heavily influenced by changing free stream direction. To find the solution which gives the total drag minimisation over the whole mission, following procedure is followed:

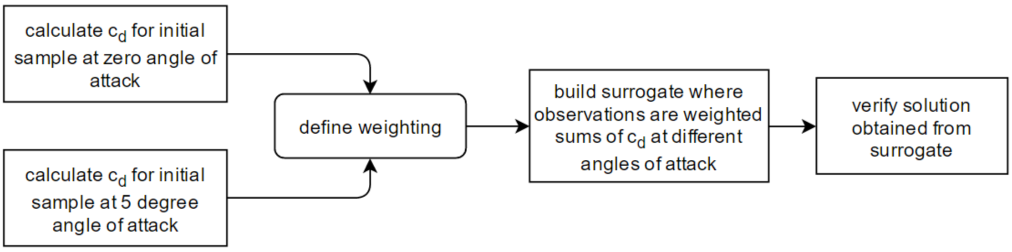

Figure 6 Scheme for search of robust aerofoil design.

The key point in finding the best design for particular problem is appropriate balance between expected flight conditions- weighting definition. This was not in the scope of the current paper, however, an example was investigated.

2.7 Results

2.7.1 Surrogate model visualisation

The results are presented on Figure 7. Results are visualised for $w_{\alpha=0} = 0.9$, $w_{\alpha=5} = 0.1$. The effect on drag coefficient, of the choice of parameters y_3 and y_4 can be observed, depending on values of y_1 and y_2. Parameters y_1 and y_2 are on the big axes, y_3 and y_4 are on horizontal and vertical axes of small subplots (not marked on Figure). The values of parameters y_1 and y_2 for subplots are $(0, 0.25, 0.5, 0.75, 1)$. For example, the central subplot represents c_d dependence on y_3 and y_4 at $(y_1, y_2) = (0.5, 0.5)$.

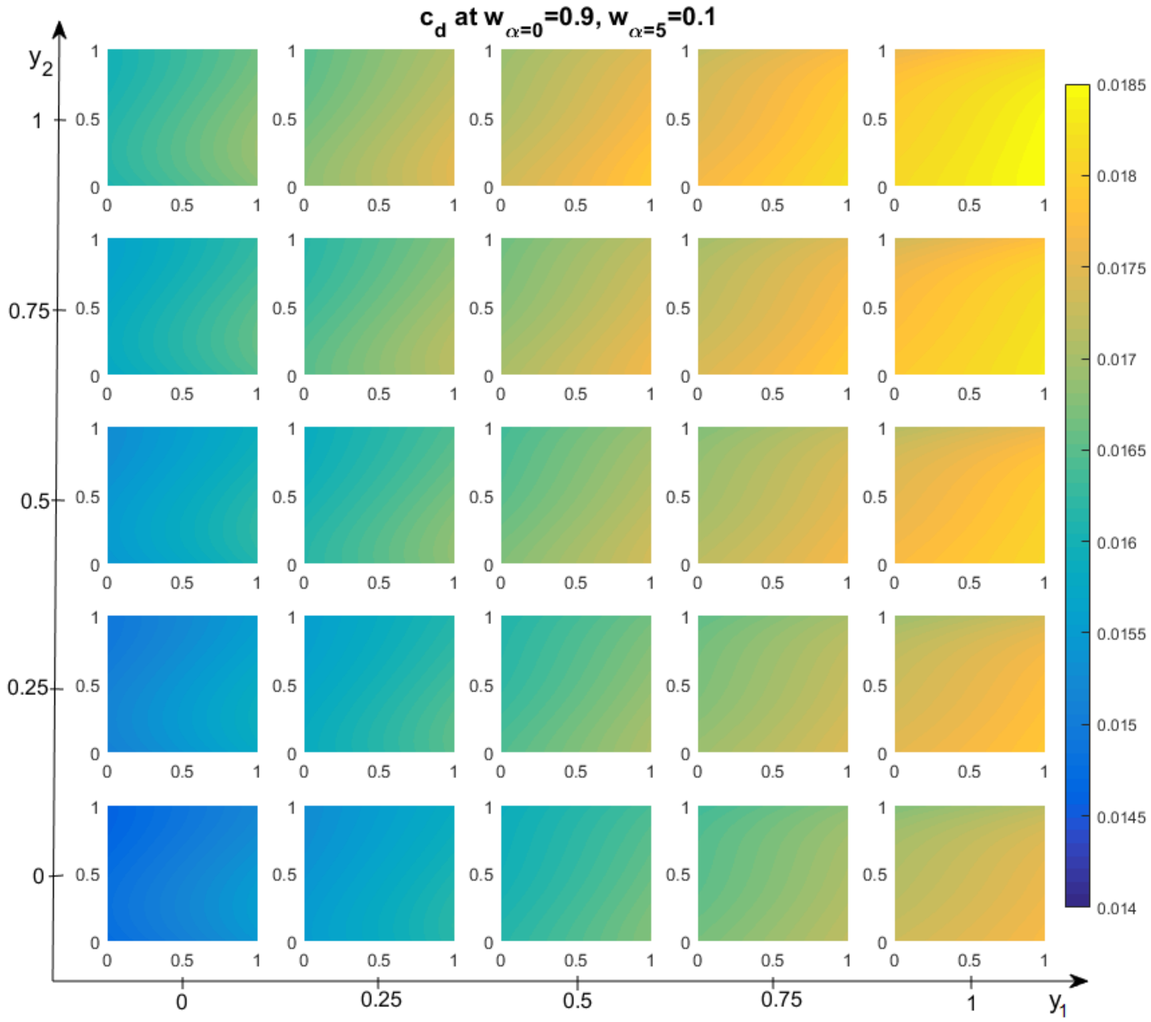

Figure 7 Surrogate visualisation of c_d predictions depending on parameters values. Parameters y_1 and y_2 are on big horizontal and vertical axes, y_3 and y_4 on horizontal and vertical axes of subplots. Subplots are created at y_1,y_2 in range (0, 0.25, 0.5, 0.75, 1).

The advantage of presenting the surrogate in this form is the ability to quickly assess the influence of individual parameters on the performance of the design. For example with y_2, y_3 and y_4 fixed, i.e. only changing y_1, c_d can vary by even 0.0024. y_2 is less effective with maximum change in c_d of 0.0014. Similarly, the effect of y_3 can be compared at different values of other parameters. For example y_3 change has slightly more effect in subplot at top left than in subplot on bottom right, which means, that at $(y_1, y_2) = (0,1)$ y_3 is more sensitive than at $(y_1, y_2) = (1,0)$.

Another advantage of building a surrogate and visualising it is the application of constraints, which were not included in the beginning. For the constraint of minimum thickness being at least 10% of chord, the constraint can be drawn on each subplot. The constraints were not included in this work, as practical engineering problem requires application of penalty function, rather than exclusion of designs, especially just below the constraint.

Finally, this from of design space analysis allows immediate determination of design robustness in terms of geometry. In this example there is no region of rapid change in c_d, which means any design is robust in terms of parameters choice, i.e. small change in geometry due to manufacturing precision, service deterioration etc. The aspect of design robustness in terms of unknown mission flight conditions, i.e. as a function of w_i can be also assessed with the use of surrogate modelling.

2.7.2 Optimised aerofoils

The resulting aerofoils are presented on Figure 8, along with NACA0010. The geometry observations are: maximum thickness in the middle, sharp leading edge and trailing edge at higher angle than in NACA0010. These tendencies for drag reduction were confirmed in literature [6]. At zero angle of attack the aerofoil tends to minimum thickness, while at 5° it is thicker than NACA0010. Important result is that the aerofoil optimised for $\alpha = 5°$ has lower c_d than NACA0010 also at $\alpha = 0$ (Figure 10).

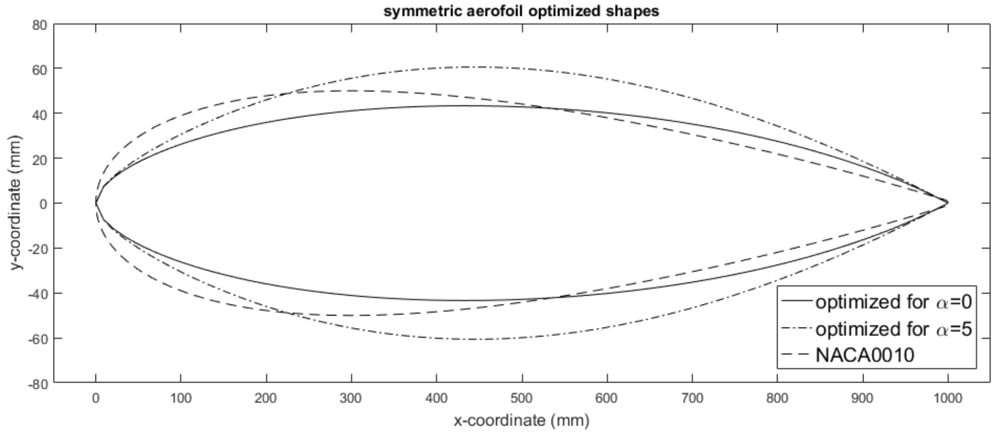

Figure 8 Results of optimisation showing optimized aerofoil geometries for two angles of attack and compared to NACA0010.

Figure 9 presents comparison of pressure coefficients for optimised aerofoils and NACA0010. Figure 5 presents pressure distribution for NACA0010 (left) and aerofoil optimised for $\alpha = 5°$ (right), for $\alpha = 0$ (top) and $\alpha = 5°$ (bottom).

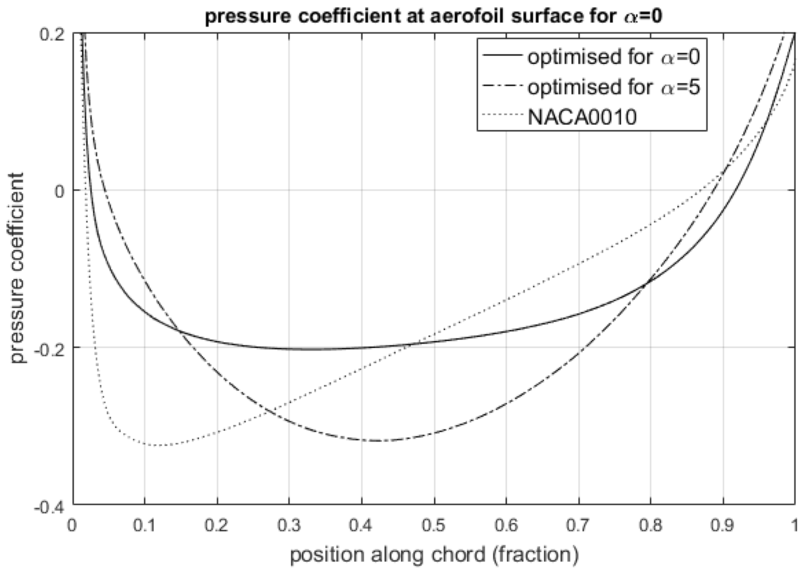

Figure 9 Pressure coefficient at the surface of optimised aerofoils and NACA0010.

Figure 10 presents the comparison of c_d at $\alpha = 0$ and $\alpha = 5°$. The designs were marked depending on satisfying of 10% chord thickness constraint. Interesting fact is that the initial sample provided many designs, dominating NACA0010 in both free stream conditions. This shows that the parametrisation was created such that most of designs within optimisation space were decent, and that optimisation space was not particularly wide.

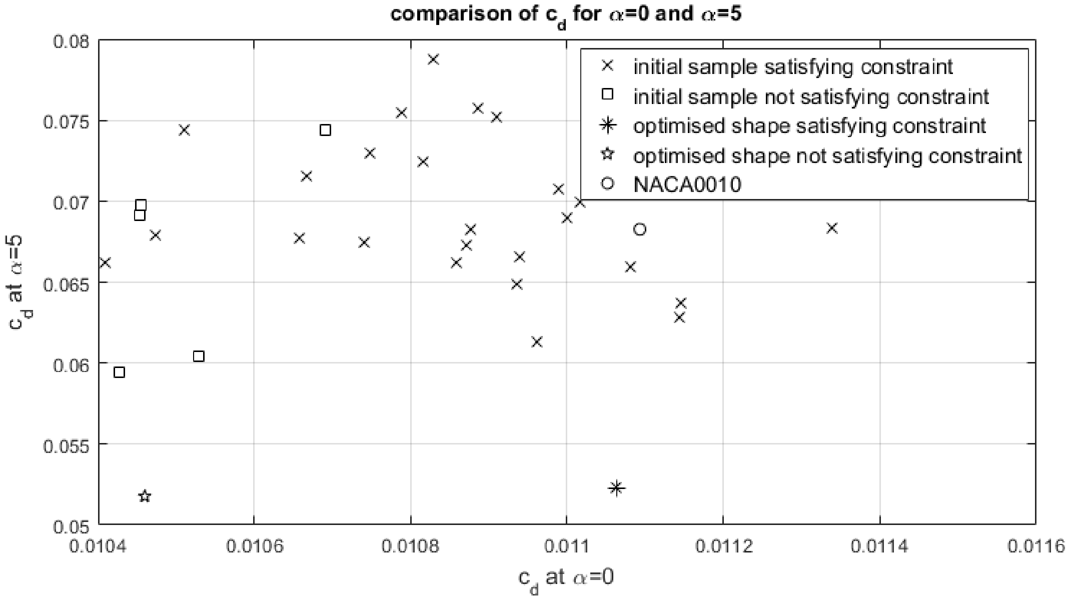

Figure 10 Graph showing drag coefficient at 0 and 5 angle of attack for all cases calculated. Best designs minimise both c_d i.e. lie in bottom left part of the graph.

3 Optimisation of asymmetric aerofoil

Asymmetric aerofoil optimisation is more complicated, due to more parameters needed for geometry definition, and multi-objective nature of problem. In case of asymmetric aerofoil, not only c_d has to be minimised, but also $\frac{c_l}{c_d}$ maximised. Objective functions are:

$$F_{1,obj} = \min[c_d(y_1, \dots, y_n)], \tag{3}$$

$$F_{2,obj} = \max\left[\frac{c_l}{c_d}(y_1, \dots, y_n)\right], \tag{4}$$

where n is number of parameters. The solution to this problem is thus not a single design, but a set of non-dominated solutions, also called Pareto front.

Following changes were made to optimisation scheme, comparing to symmetric aerofoil case:

1. **Parametrisation**. Just like in symmetric aerofoil case, 4 guide points were used to create each of two NURBS curves: upper and lower surface (Figure 11). Additionally, a parameter defining angle between chord line and free stream was needed. This gave 9 parameters defining the problem.

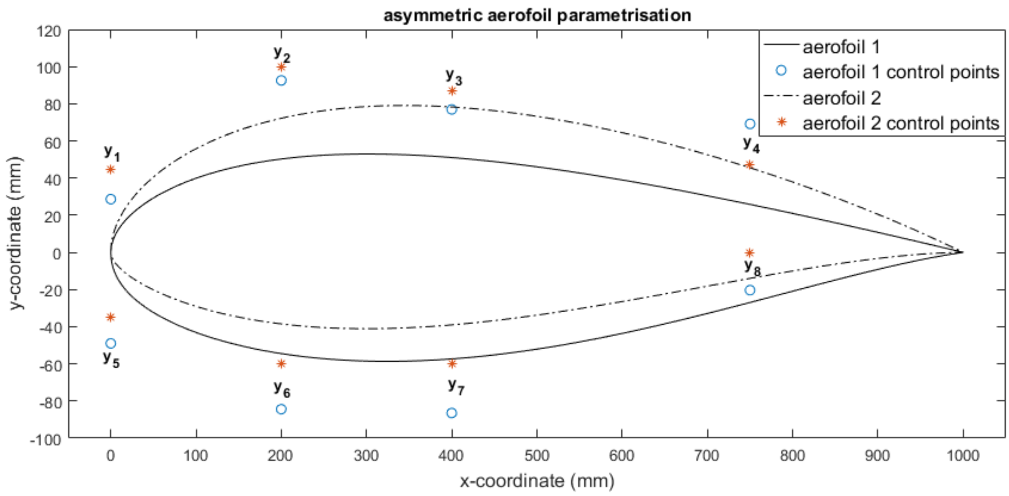

Figure 11 Asymmetric aerofoil parametrisation using 8 parameters for shape and 9th for angle of attack.

2. **Design of experiments**. Symmetric aerofoil surrogate model from previous section was very accurate, predicting c_d very precisely. It was built with $10n$ sample points. It was thus reasonable to reduce the size of initial sample to 60 points (for 9 parameters). It was expected that with such a reduction, the quality of the surrogate model would not match that of previous case, however, the surrogate was only needed to guide optimisation, not give exact predictions at any point.

The rest of steps were exactly the same as in the case of symmetric aerofoil, with the only difference of fitting the surrogate through varying angle of attack, instead of running multiple simulations for each geometry.

3.1 Results

The surrogate model built using initial 60 points, gives multiple solutions for maximisation of lift-to-drag ratio up to 53. The model was exploited in these areas, by feeding the surrogate with 10 points of predicted optima, resulting in a range of similar $\frac{c_l}{c_d}$ values and varying c_d (Figure 12). The model's expected minimum c_d design was verified, however, it was not as good as expected- giving around 10% higher c_d than those found in symmetric aerofoil case. The next step was finding Pareto front.

3.2 Search for Pareto front

Following procedure was developed to search for the set of non-dominated designs:

1. Scale c_d to the same order of magnitude as $\frac{c_l}{c_d}$, and the same optimisation goal, i.e. maximisation, by applying the formula:

$$f_{c_d} = \left| \left(\frac{c_l}{c_d}\right)_{max} - c_d \times \frac{\left(\frac{c_l}{c_d}\right)_{max}}{c_{d_{max}}} \right|, \tag{5}$$

where $(\frac{c_l}{c_d})_{max}$ and $c_{d_{max}}$ were the surrogate model predictions. In this case their values were taken as 50 and 0.2 respectively. f_{c_d} is a measure of drag coefficient, scaled to $\frac{c_l}{c_d}$, such that values it took, were between 0 (for maximum c_d) and 50 (for minimum c_d).

2. Having both objective functions in the same form (range of 0 to 50 and , a weighting, which combines both measures, can be built, which returns the surrogate model prediction of the most optimal single objective $f_{s,obj}$ of the form:

$$f_{s,obj} = w_1 \times \frac{c_l}{c_d} + (1 - w_1) \times f_{c_d}, \tag{6}$$

where w_1 is weighting of lift-to-drag ratio, $0 \leq w_1 \leq 1$.

3. $f_{s,obj}$ were calculated for $w_1 = (0, 0.1, \dots, 1)$, i.e. 10 cases. The resulting designs were verified by black-box, and compared to initial sample, and designs found in previous section (exploitation of the surrogate). All results are presented on Figure 12.

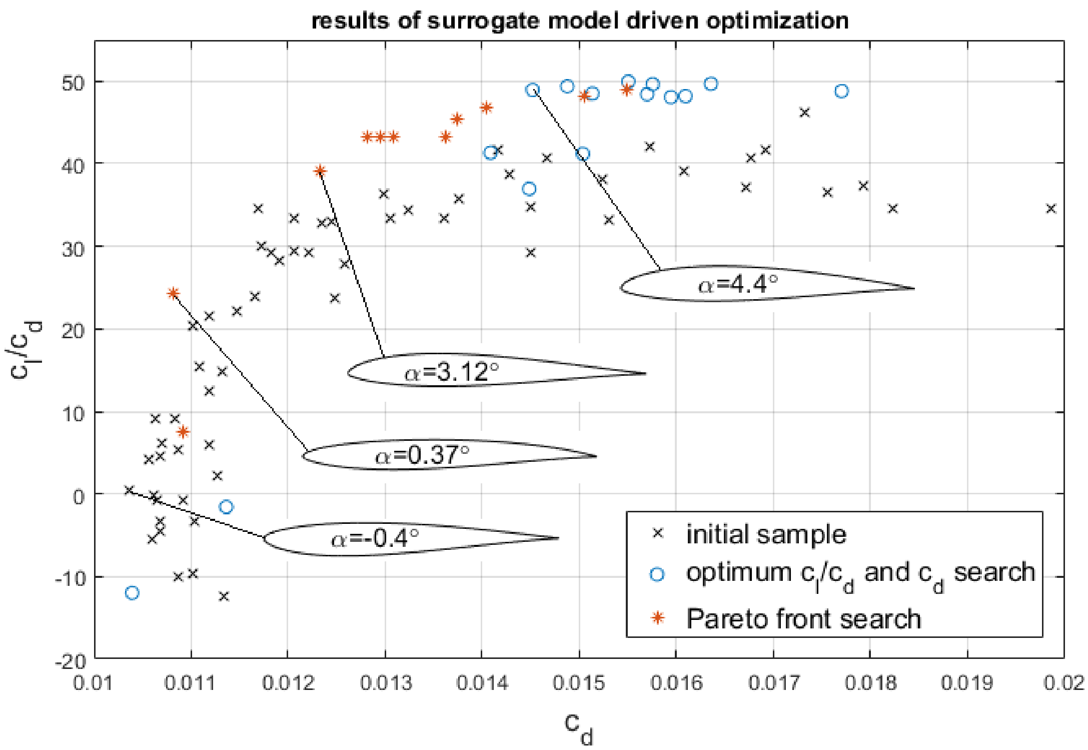

Figure 12 Graph showing results of surrogate model driven optimisation with chosen results..

It can be observed, that even though the approach for finding Pareto front was intuitive, a few new, non-dominated designs were found. The accuracy of this approach is limited by the surrogate model quality. As expected, lower w_1, means lower c_d, $\frac{c_l}{c_d}$ and α. It should be also noted, that Pareto front was well determined for $\frac{c_l}{c_d} > 35$, and for lower values it is missing expected results. For $w_1 = 0$ it was expected to obtain symmetric, thin aerofoil, at $\alpha = 0$, as was found in previous section (symmetric aerofoil optimisation). The resulting c_d for $\frac{c_l}{c_d} = 0$ was below 0.01. In this case- 0.014. If low c_d and $\frac{c_l}{c_d}$ is the area of interest of designer, more exploration and exploitation of the surrogate should be done, like it was shown for high $\frac{c_l}{c_d}$.

4 Applications to empennage robust design

The design process of empennage can take different forms, the presented approach assumes an aerofoil is picked independently of planform, exact position etc.. The needed knowledge is the layout (Figure 13), and direction of lift needed for stability in straight flight (upwards or downwards). If the layout is to be chosen, basing on possible aerofoil characteristics, they should be quickly assessed, and this paper addresses this approach as well.

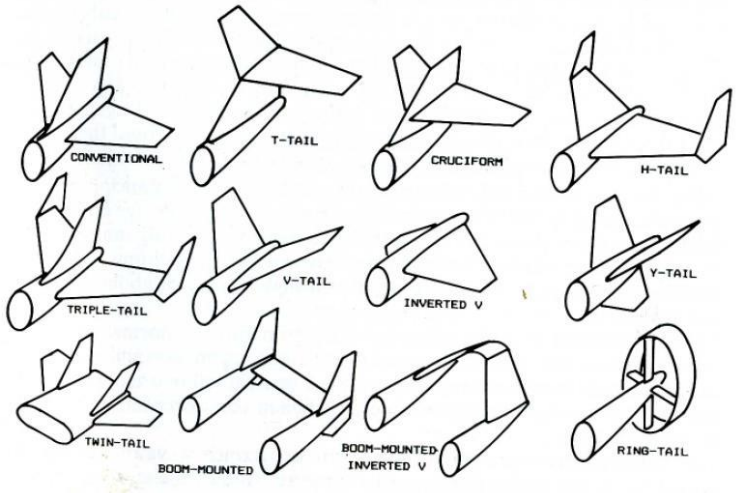

Figure 13 Most popular empennage layouts [11].

Further development of the empennage is directed at 3D wing synthesis, more realistic flow definition, accounting for interference etc.

Current “Samonit” empennage is a boom-mounted v-tail with simple rectangular planform. Depending on the mission scenario, the weightings of angle of attack for symmetric aerofoil can be chosen to find the most optimal shape. If mission scenario is not fixed, a trade-off between maximum drag reduction and robustness can be made. On the other hand, knowing the aerofoil (both symmetric and asymmetric) characteristics, a comparison between v-tail and conventional tail can be made, for particular mission.

5 Conclusion

In the current paper a very quick optimisation procedure, for finding a robust aerofoil, was presented. With the number of direct CFD analyses of less than 100, it was shown that an aerofoil, being considerably better than example NACA aerofoil, can be found. Thanks to a very low number of CFD analyses, high fidelity RANS could be used. The methodology presented in this paper gives aerofoil for particular surface of empennage layout chosen, or can be used as a help, in finding the optimal empennage layout, considering the varying flight conditions.

5.1 Limitations of performed optimisation

Parametrisation. There are two problems concerning parametrisation used in this work. Firstly, few parameters were picked to define the geometries. There are clearly many geometries impossible to create with such parametrisations. The second problem was narrow limit on upper and lower boundaries. The resulting optimal geometries were defined with parameters values lying on the boundary, i.e. 0 or 1. It can be expected that more optimal design would be found by reducing/increasing further the parameter.

Analysis and black-box. The choice of analysis- 2D does not account for very important drag component- induced drag. The next limitation of the analysis method is, that it assumed no upstream interference from aircraft main wing and fuselage. Of all computational methods, however, the used one is of the highest fidelity, so only wind tunnel testing can reduce the error in observations.

Surrogate model accuracy (asymmetric case). The quality of surrogate model created for asymmetric case proved that more points are needed for good prediction of design space. Although some regions were accurate, the surrogate prediction of maximum lift-to-drag ratio was overestimated by 3-5%. On the other hand the surrogate prediction gave a few good designs forming Pareto front, and guided the optimisation to obtain good results.

References

[1] Forrester, A., Sobester, A., & Keane, A. (2008). *Engineering design via surrogate modelling: a practical guide*. John Wiley & Sons.

[2] Forrester, A. I., & Keane, A. J. (2009). Recent advances in surrogate-based optimization. *Progress in Aerospace Sciences, 45(1),* 50-79.

[3] Goraj, Z., Cisowski, J., Frydrychewicz, A., Grendysa, W., Jonas, M. (2008b), Mini UAV design and optimization for long endurance mission, Proceedings of ICAS Congress 2008, ICAS, Anchorage, paper 437, Sept.2008.

[4] Goraj, Z., Rodzewicz, M., Grendysa, W., Jonas, M. (2012), Design and configuration layouts of an advanced long endurance UAV- lessons learnt after flight testing. ICAS Congress 2012, Brisbane, paper 763, Sept.2012.

[5] Keane, A., & Nair, P. (2005). *Computational approaches for aerospace design: the pursuit of excellence.* John Wiley & Sons.

[6] Kontogiannis, S. G., & Ekaterinaris, J. A. (2013). Design, performance evaluation and optimization of a UAV. *Aerospace Science and Technology,29(1),* 339-350.

[7] Li, W., Huyse, L., & Padula, S. (2002). Robust airfoil optimization to achieve drag reduction over a range of mach numbers. *Structural and Multidisciplinary Optimization*, *24*(1), 38-50.

[8] Mullen, Benjamin J., and Sebastian Lachance-Barrett. "FLUENT-Flow over an Airfoil." FLUENT. Cornell University, 09 Feb. 2014. Web. 13 July 2016. <https://confluence.cornell.edu/display/SIMULATION/FLUENT+-+Flow+over+an+Airfoil>.

[9] Panagiotou, P., Kaparos, P., & Yakinthos, K. (2014). Winglet design and optimization for a MALE UAV using CFD. *Aerospace Science and Technology,39,* 190-205.

[10] Peigin, S., & Epstein, B. (2004). Robust optimization of 2D airfoils driven by full Navier–Stokes computations. *Computers & fluids, 33(9),* 1175-1200.

[11] Raymer, D. P. (1999). *Aircraft Design: A Conceptual Approach*. Reston, VA: American Institute of Aeronautics and Astronautics.

[12] Ribeiro, A. F., Awruch, A. M., & Gomes, H. M. (2012). An airfoil optimization technique for wind turbines. *Applied Mathematical Modelling, 36(10),* 4898-4907.

[13] Sóbester, A., & Forrester, A. I. (2014). *Aircraft aerodynamic design: geometry and optimization*. John Wiley & Sons.

[14] Tsutsui, S., & Ghosh, A. (1997). Genetic algorithms with a robust solution searching scheme. *IEEE transactions on Evolutionary Computation, 1(3),* 201-208.

[15] Wang, Y. Y., Zhang, B. Q., & Chen, Y. C. (2011). Robust airfoil optimization based on improved particle swarm optimization method. *Applied Mathematics and Mechanics, 32,* 1245-1254.

[16] Wickramasinghe, U. K., Carrese, R., & Li, X. (2010, July). Designing airfoils using a reference point based evolutionary many-objective particle swarm optimization algorithm. In *IEEE Congress on Evolutionary Computation (pp. 1-8). IEEE*.

[17] Yeniay, Ö. (2005). Penalty function methods for constrained optimization with genetic algorithms. *Mathematical and Computational Applications, 10(1),* 45-56.

[18] Zetina, A. M., Jeong, S., & Obayashi, S. (2013, June). Airfoil aerodynamic optimization for a high-altitude long-endurance aircraft using multi-objective genetic-algorithms. In *2013 IEEE Congress on Evolutionary Computation (pp. 2314-2320). IEEE*.